Received: 18 May 2019 | Revised: 28 June 2019 | Accepted: 18 July 2019

DOI: 10.1111/cas.14143

ORIGINAL ARTICLE

Cancer Science WILEY

A novel pan-cancer biomarker plasma heat shock protein 90alpha and its diagnosis determinants in clinic

Wei Liu[1,2,3] | Jie Li[4] | Ping Zhang[1] | Qiaoyun Hou[1,2,3] | Shi Feng[1,2,3] | Lisheng Liu[5] | Dawei Cui[1] | Hubing Shi[6] | Yan Fu[1,2,3] | Yongzhang Luo[1,2,3]

[1]The National Engineering Laboratory for Anti-Tumor Protein Therapeutics, Tsinghua University, Beijing, China

[2]Beijing Key Laboratory for Protein Therapeutics, Tsinghua University, Beijing, China

[3]Cancer Biology Laboratory, School of Life Sciences, Tsinghua University, Beijing, China

[4]Beijing Chest Hospital, Capital Medical University, Beijing, China

[5]Clinical Laboratory, Shandong Cancer Hospital, Jinan, China

[6]Laboratory of Tumor Targeted and Immune Therapy, Clinical Research Center for Breast, State Key Laboratory of Biotherapy, West China Hospital, Sichuan University and Collaborative Innovation Center, Chengdu, China

Correspondence
Yongzhang Luo, School of Life Sciences, Tsinghua University, Beijing 100084, China.
Email: yluo@mail.tsinghua.edu.cn

Funding information
Protgen Ltd; National Key R&D Program of China, Grant/Award Number: 2016YFC0906000 and 2016YFC0906003

Abstract

A sensitive and specific diagnosis biomarker, in principle scalable to most cancer types, is needed to reduce the prevalent cancer mortality. Meanwhile, the investigation of diagnosis determinants of a biomarker will facilitate the interpretation of its screening results in clinic. Here we design a large-scale (1558 enrollments), multicenter (multiple hospitals), and cross-validation (two datasets) clinic study to validate plasma Hsp90α quantified by ELISA as a pan-cancer biomarker. ROC curve shows the optimum diagnostic cutoff is 69.19 ng/mL in discriminating various cancer patients from all controls (AUC 0.895, sensitivity 81.33% and specificity 81.65% in test cohort; AUC 0.893, sensitivity 81.72% and specificity 81.03% in validation cohort). Similar results are noted in detecting early-stage cancer patients. Plasma Hsp90α maintains also broad-spectrum for cancer subtypes, especially with 91.78% sensitivity and 91.96% specificity in patients with AFP-limited liver cancer. In addition, we demonstrate levels of plasma Hsp90α are determined by ADAM10 expression, which will affect Hsp90α content in exosomes. Furthermore, Western blotting and PRM-based quantitative proteomics identify that partial false ELISA-negative patients secret high levels of plasma Hsp90α. Mechanism analysis reveal that TGFβ-PKCγ gene signature defines a distinct pool of hyperphosphorylated Hsp90α at Theronine residue. In clinic, a mechanistically relevant population of false ELISA-negative patients express also higher levels of PKCγ. In sum, plasma Hsp90α is a novel pan-cancer diagnosis biomarker, and cancer diagnosis with plasma Hsp90α is particularly effective in those patients with high expression of ADAM10, but may be insufficient to detect the patients with low ADAM10 and those with hyperphosphorylated Hsp90α.

KEYWORDS
ADAM10, heterogeneity, Hsp90α, pan-cancer biomarker, PKCγ

1 | INTRODUCTION

An accurate diagnosis biomarker, in principle for different types of cancer, is an alternative but economical way to prevent worldwide cancer deaths. Blood-based liquid biopsy represents a promising non-invasive clinical method for cancer detection. Increasing reports have focused on circulating tumor cells (CTCs), circulating tumor DNA (ctDNA), serum noncoding RNAs, or exosomes as a way to identify tumor-associated biomarkers.[1] Emerging studies have attempted to integrate blood biomaterials to all-in-one biosources to detect patients with pan-cancer diseases. Initial studies have shown that ctDNA was detectable in >75% patients with multiple advanced cancer diseases, but in <50% patients with local diseases.[2] A subsequent study suggested that RNA-seq of tumor-educated platelets achieved 96% accuracy for the detection of patients with multiclass cancers.[3] Papadopoulos's group developed a test called CancerSEEK, which combined the mutation of cell-free DNA and circulating proteins, and detected a median of 70% of eight cancer types.[4] However, limitations, including the absence of healthy controls or patients with at-risk diseases and no independent validation dataset, should be noted in stating these results. In addition, the involved technologies, referring to expensive high-throughput sequencing platforms and data analyses with support vector machines or other bioinformatics methods, often required highly experienced experts to operate the equipment and explain the data, which hampers its translation to the clinic. Until this time, early detection of patients with cancer is critical, and a clinical usable detection platform is urgently needed.

Heat shock protein 90alpha (Hsp90α), a well studied molecular chaperone involved in stress tolerance, has recently been found to localize outside various cancer cells.[5] Extracellular Hsp90α (eHsp90α) can promote cell invasion[6] and epithelial-to-mesenchymal transition (EMT) processes[7] in multiple cancer cells. Clinical trials have demonstrated that plasma Hsp90α is a more accurate diagnostic biomarker compared with commonly used biomarkers carcinoembryonic antigen (CEA) and fragments of cytokeratin-19 (CYFRA21-1) in lung cancer,[8] or alpha-fetoprotein (AFP) in liver cancer,[9] respectively. In the clinic, a quantitative ELISA kit for plasma Hsp90α has now been approved by the China Food and Drug Administration (CFDA) to be used for patients with lung or liver cancers (see http://www.sfda.gov.cn). Ongoing clinical trials, including with patients with colorectal or breast cancer, also showed that plasma Hsp90α is a much more precise diagnostic biomarker (to be published). Together, this evidence provides a strong rational to generalize the quantitation of plasma Hsp90α based on ELISA in the diagnosis of patients with multiclass cancer. If confirmed, this approach will represent plasma Hsp90α as a novel pan-cancer diagnostic biomarker. Therefore, we designed a large-scale, multicenter, and cross-validation study to assess the diagnostic accuracy of plasma Hsp90α as a biomarker for pan-cancer diseases.

After a potential biomarker has been translated into the clinic, there is almost no research to investigate the diagnostic determinants of the new or already existing tumor biomarkers.[10,11] This situation makes it impossible to address causes and anticipated risks of outlier samples identified in the clinic such as limited sensitivities or patients with cancer identified erroneously as healthy individuals. We propose that the diagnostic performance is often limited to a poor understanding of the biology of a biomarker. Taking plasma Hsp90α as an example, two aspects should be considered to explain its diagnostic capability as a biomarker in the clinic: first, is to confirm whether plasma Hsp90α is actually secreted in ELISA-negative patients. Regarding this point, we need to understand thoroughly the upstream regulator controlling its secretion into the blood; and the second is to investigate whether the recognition ability of the antibody in the ELISA kit will be compromised by the heterogeneity of secreted Hsp90α. This aspect will lead to false ELISA-negative patients. As a result, we have investigated systematically determinants that could affect the diagnosis performance of plasma Hsp90α.

2 | MATERIALS AND METHODS

2.1 | Study design and participants in diagnosis

We conducted a prospective and tentative diagnosis study (e-CAF: an early, Convenience, Accuracy, and Fast, pan-cancer diagnosis biomarker for patients with cancer) using an ELISA kit to measure quantitatively plasma Hsp90α from patients with different types of cancer. All these studies conformed to the provisions of the Declaration of Helsinki. The study was approved by the Institutional Review Board of Tsinghua University, China.

2.1.1 | Participants enrolled in the test cohort

In the test cohort, 628 participants, consisting of 300 patients with different types of cancer (including liver, lung, breast, colorectal, stomach, pancreatic, esophagus cancer, and lymphoma), 196 patients with common at-risk diseases (referring to chronic hepatitis, tuberculosis, benign lung tumor, colon polyps, mastitis), and 132 healthy individuals, were enrolled from hospitals from May 2009 through to September 2015. Three populations, including healthy individuals, patients with at-risk diseases, and patients with cancer, were separated by medical doctors. The diagnosis of different cancer diseases was confirmed histologically by corresponding pathologists. Blood samples of jaundice, hemolysis, and lipemia, were excluded from the test cohort. The study was approved by the local research ethic committees. Written informed consents from all participants were obtained under regulations from the First Affiliated Hospital of Zhejiang University (Zhejiang, China), Zhejiang Province People's Hospital (Zhejiang, China), Shandong Cancer Hospital (Jinan, China), and Beijing Chest Hospital (Beijing, China).

2.1.2 | Data compiling in validation cohort

Project e-CAF was conducted on four individual cancer indications in clinical trials, including breast (registered at ClinicalTrial.gov:

NCT02324101), lung (registered at the National Medical Products Administration (NMPA), China),[8] liver (registered at ClinicalTrial.gov: NCT02324127),[9] and colorectal cancer (registered at ClinicalTrial.gov: NCT02324114). To validate our observations in the test cohort, we compiled a validation dataset from curated data in project e-CAF, according to probability theory. With the help of the random number generator in R (version 3.5.0), 672 enrollments, including 361 patients with corresponding cancer types, 112 patients with different non-cancerous diseases, and 199 healthy individuals, were randomly compiled and defined as the validation cohort. In these patients with cancer, tumor staging was determined according to the tumor, node, metastasis (TNM) staging system,[12] of which stage I and stage II were classified as patients with early-stage cancers.

Clinical data of other biomarkers, including AFP, CEA, CA19-9, and CA-125, in 112 patients with cholangiocarcinoma, or combined hepatocellular carcinoma and cholangiocarcinoma, were also extracted from project e-CAF for patients with liver cancer.[9]

2.2 | Small-scale lung or colorectal patients enrollment

To confirm the relationship between the high expression of ADAM10 and the elevated secretion of plasma Hsp90α, 30 patients with lung or colorectal cancer were recruited from Beijing Chest Hospital, Capital Medical University, and West China Hospital, Sichuan University, respectively, from July 2017 to June 2018. The diagnosis of patients with corresponding different types of cancer was confirmed histologically by the pathologists. All patients signed an informed consent approved by the local review committee from Sichuan University and Beijing Chest Hospital.

2.3 | Quantification of plasma Hsp90α by ELISA

ELISA detection of plasma levels of Hsp90α was performed as described previously.[9] Briefly, peripheral blood samples (EDTA-K2 anticoagulant) from all participants were collected and then stored at −20°C, until use. We used a commercially available ELISA kit (Protgen) for the quantitative measurement of plasma Hsp90α, according to the manufacturer's recommendations. The kit was equilibrated for 30 min at 37°C. The solution was thoroughly mixed before use to avoid the formation of foam. Concentrated wash buffer was diluted with 475 mL deionized water and mixed thoroughly. The standard was reconstituted with 0.4 mL sample diluent and mixed thoroughly. Samples were diluted 20-fold with the diluent. Next, 50 μL of standard or diluted sample and 50 μL HRP-conjugate reagent were added to each well and mixed gently by shaking. The plate was covered with a membrane (microplate sealer) and incubated at 37°C for 1 h. The liquid was discarded and 300 μL wash buffer was added to each well manually or with a plate washer. This procedure was repeated for six washes. After the final wash, the plate was inverted and blot dried by banging the plate onto absorbent paper. Next, 50 μL chromogen solution A and 50 μL chromogen solution B were added to each well, and mixed gently by shaking, and incubated (away from light) at 37°C for 20 min. The reaction was stopped by adding 50 μL stop solution to each well, and the absorbance read (optical density, OD) at 450 nm/630 nm using a microplate reader within 10 min of adding the stop solution. A standard curve was generated by plotting on the vertical (*Y*) axis the logarithm of the average OD obtained for each of the six standards versus the logarithm of corresponding concentrations on the horizontal (*X*) axis. To determine the amount of Hsp90α in each sample, absorbance for the samples was then substituted in the regression equation standard curve. Double logarithmic curve fitting was recommended, and the coefficient of correlation (R^2) was required to be >0.980.

2.4 | Library preparation for RNA-seq

Total RNA was isolated from different subclonal populations using TRIzol reagent (Invitrogen). The quality of extracted RNA was determined using capillary electrophoresis on a Bioanalyzer 2100 instrument (Agilent Technologies). mRNA with a polyA tail was enriched using oligo(dT) magnetic beads, followed by DNase I (Invitrogen) incubation to remove genomic DNA. The target mRNA was fragmented and reverse transcribed into double-strand cDNA (dscDNA) using N6 random primers. After end repair with phosphate at the 5′ end and addition of "A" nucleotides at 3′ end, dscDNA was ligated with an adaptor containing "T" nucleotides at the 3′ end of the dscDNA. Next, ligation products were amplified with two specific primers; and the PCR product was denatured by heat, and the single-strand DNA cyclized (ssDNA circle) with a splint oligo and DNA ligase. Quality and quantity were confirmed by high sensitivity DNA assay on a Bioanalyzer 2100 instrument (Agilent Technologies). Library sequencing was then performed using a combinatorial probe-anchor synthesis (cPAS)-based BGISEQ-500 sequencer (BGI). Base calling was carried out with in-house BGISEQ-500 software.

2.5 | Bioinformatics analysis

2.5.1 | Differentially expressed gene analysis from various cancers versus corresponding normal tissues

Expression profiling for a specific type of cancer and corresponding normal tissues were all downloaded from the Gene Expression Omnibus (GEO).[13] Differentially expressed genes (DEGs) in each dataset were analyzed separately using the integrated GEO2R web tool (https://www.ncbi.nlm.nih.gov/geo/info/geo2r.html) as different platforms or normalization standards might have been used when gene expression was profiled. Each sample within a GEO series was first classified into either normal tissue or tumor tissue, then the defined groups were input into GEO2R. GEO2R provided a list of DEGs ranked according to differential expression levels. Gene probes lacking gene symbols were excluded from the adjusted list. A GEO series in which the number of calculated DEGs was <100 was also omitted from the subsequent meta-analysis. To gain further insight into the general mechanism underlying the secretion

of Hsp90α, multiple lists of DEGs from different cancer types were input into Metascape[14] to analyze overlapping genes and shared signaling pathways from the different cancer types.

2.5.2 | RNA-seq analysis

Raw reads were first subjected to quality control, including removal of adaptors and trimming of reads with unknown bases <10% and reads with >50% low-quality bases. After filtering, clean reads were stored as FASTQ file format.[15] Bowtie[16] and HISAT[17] software were used to align clean reads to the reference genome. The fragments per kilobase of transcript per million mapped reads (FPKM) method integrated in RSEM[18] was used to calculate the expression levels of the genes. DEGs were screened using the DESeq2 method[19] with a default criteria fold change ≥ |2| and diverge probability ≥ 0.8. To gain further insight into the biological pathways resulting in eHsp90α heterogeneity, gene set enrichment analysis (GSEA) was performed. The gene sets with a false discovery rate (FDR) of 0.25 were considered enriched between classes in comparison. Gene Ontology (GO) gene sets for biological process database (c5.bp.v6.1.symbols.gmt) from the Molecular Signature Database v6.2 were used for enrichment analysis. Gene set of <15 genes were excluded from the analysis.

2.5.3 | Upstream regulator analysis of singe clone 6A5 versus 13B5

Upstream transcription factors (TFs) usually regulate the expression of multiple downstream genes. To characterize upstream TFs, DEGs between clone 6A5 and 13B5 were analyzed using QIAGEN's Ingenuity® Pathway Analysis software (IPA®, QIAGEN Redwood City, www.qiagen.com/ingenuity). Comparing DEGs in the Ingenuity® Knowledge Base, a list of upstream regulators based on connectivity was obtained. Only genes with a fold change of |2| and *P*-value < .05 were considered. Based on the calculated overlap *P*-value (Fisher's exact test) and an activation *z* score, only results with an FDR-q < 0.05 and a *z* score > |2| were considered significant.

2.6 | Fluorescence activated cell sorting (FACS) analysis for single cell isolation

MCF7-GFP, A549-GFP, H1299-GFP, and MDA-MB-231-GFP, were collected and suspended in FACS buffer (phosphate-buffered saline [PBS] with 1% fetal bovine serum [FBS] and 2 mmol/L EDTA). GFP-positive cells were sorted into 96-well plates using a BD FACS Aria III instrument (BD Biosciences) for further culture and subsequent study.

2.7 | Cell culture, RNA interference, qRT-PCR, antibodies, reagents

2.7.1 | Cell culture

All cell lines were purchased from the American Type Culture Collection. MCF-7, A549, PANC1, H1299, MDA-MB-231, Hela, HepG2, and HEK293T were maintained in Dulbecco's modified Eagle's medium (DMEM) supplemented with 10% FBS, 100 U/mL penicillin, and 100 μg/mL streptomycin (HyClone). HaCat and MDA-MB-231 were cultured in RPMI 1640 medium also supplemented with 10% FBS, 100 U/mL penicillin, and 100 μg/mL streptomycin (HyClone).

2.7.2 | Antibodies and reagents

Antibodies were purchased from commercial sources: rabbit anti-phosphoserine-protein kinase C (PKC) substrate (#2261) and anti-phosphothreonine (#9386) antibodies were purchased from Cell Signaling Technology; rabbit anti-PKCγ from Santa Cruz Biotechnology; mouse anti-phosphoserine (#2023922) and rabbit anti-acetylation antibodies (#06-933) were obtained from Millipore; rabbit anti-HA (hemagglutinin) (ab9110), anti-ADAM10 (ab1997), and anti-Hsp90α (ab2928) antibodies were purchased from Abcam; anti-actin antibody (CW0096M) was bought from CWBIO; horseradish peroxidase-conjugated goat anti-mouse or rabbit antibodies were obtained from Abmart. Protein A/G agarose and protease and phosphatase inhibitors (Complete™ Protease Inhibitor Cocktail tablets and PhosSTOP phosphatase Inhibitor Cocktail tablets) were purchased from Roche. The inhibitor for ADAM10 GI254023X was purchased from Sigma-Aldrich.

2.7.3 | Reverse transcription and quantitative real-time PCR (qRT-PCR)

Total RNA was extracted from cell pellets using TRIzol reagent (Invitrogen). cDNA was synthesized using a RevertAid First Strand cDNA Synthesis Kit (Invitrogen). qRT-PCR was carried out to measure mRNA levels. The reaction system consisted of 20 μL reaction mixtures containing TransStart Green qPCR SuperMix (TransGen Biotech), 6 pmol of each primer, and cDNA. The reaction was run on the Mx3000P system (Stratagene). The mRNA expression level of glyceraldehyde 3-phosphate dehydrogenase (GAPDH) was used as the internal control. The cycling program was as follows: initial denaturation at 96°C for 2 min, 25 rounds of 96°C for 30 s, corresponding annealing temperature for 15 s, and 72°C for 30 s, followed by a final 72°C elongation step for 5 min. Relative quantification was performed using the $\Delta\Delta C_T$ method.

2.8 | Immunoprecipitation

Cells were lysed in ice-cold NP-40 lysis buffer (50 mmol/L Tris-HCl at pH 8.0, 150 mmol/L NaCl, 1% NP-40, protease inhibitors cocktail; Roche). Lysates were centrifuged for 10 min at 16 000 *g* at 4°C. Supernatants were recovered and incubated with primary antibodies for more than 4 h at 4°C. Protein A/G agarose resin (Roche) was added to the mixture and tumbled in a tube rotator overnight at 4°C. The immunoprecipitates bound to the resin were washed five times with lysis buffer, then re-suspended in sample loading buffer, and resolved by SDS-PAGE.

2.9 | Mini-scale siRNA screening

Independent siRNA targeting candidate genes were designed and synthesized (GenePharma). For transient transfection, cells at 50%-70% confluence were transfected in 6-well plates with Lipofectamine 3000 reagent (Invitrogen) following the designated protocol. Scramble non-targeting siRNAs (GenePharma) were used as the mock control. After 24-48 h post transfection, culture medium was changed for another 16 h, then the cells and conditioned medium were collected for further analysis. shRNA vectors for stable knockdown of ADAM10 were obtained from the Center of Biochemical Analysis, Tsinghua University.

2.10 | In vitro phosphorylation of rHsp90α by PKCγ

An in vitro PKCγ phosphorylation assay for rHsp90α was performed as described.[20] Briefly, recombinant Hsp90α and PKC were incubated together in PKC reaction buffer (20 mmol/L Hepes [pH 7.4], 1.67 mmol/L CaCl2, 10 mmol/L MgCl2, and 1 mmol/L DTT) with or without ATP for 60 min. Then, samples were subjected to western blotting and ELISA for further analysis.

2.11 | Immunofluorescence

For immunofluorescence to detect the colocalization of ADAM10 and Hsp90α, cells were seeded onto coated coverslips in 24-well plates overnight, fixed with 4% paraformaldehyde for 10 min at room temperature, and blocked with 10% goat serum for 60 min at room temperature, followed by incubation with indicated primary antibodies. Corresponding secondary antibodies labeled with different fluorochromes were used to visualize the target proteins. Images were acquired and analyzed using a Nikon A1 confocal microscope (Nikon).

2.12 | Immunohistochemistry (IHC)

Immunohistochemistry (IHC) was performed as described previously.[21] Briefly, to detect the expression of ADAM10 in a human cancer tissue microarray (MC2081a, Alenabio) and in animal tissue, tumor tissue slides were probed with primary antibodies at indicated concentrations overnight at 4°C, followed by incubation with HRP-conjugated secondary antibody at room temperature for 1 h. Chromogenic 3,3′-diaminobenzidine (DAB) substrate was added to visualize the expression of the target proteins.

2.13 | Western blotting

Western blotting assays were performed as described in detail.[21] Cells were scraped off the culture plates, and washed twice with PBS. After centrifugation, cell pellets were collected, denatured with loading buffer, boiled for 15 min, and separated on 10% SDS-PAGE gels, followed by transfer to polyvinylidene difluoride (PVDF) membranes. The target proteins were probed with the indicated primary antibodies overnight at 4°C, then incubated with horseradish peroxidase (HRP)-conjugated secondary antibodies for 1 h at room temperature, and visualized using a common enhanced chemiluminescence technique (Beyotime) according to the manufacturer's protocol.

2.14 | Animal studies

All animal studies were approved by the Institutional Animal Care and Use Committee of Tsinghua University. Mice were housed in AAALA-approved laboratory animal care facilities. A549 and PANC1 cells (5×10^6 cells per mouse) stably knocking down ADAM10 mixed with Matrigel 1:1 were injected subcutaneously into 6-wk-old mice. After 2 wk, mice were sacrificed and primary tumor tissues were embedded in paraffin, sectioned and applied for immunohistochemistry (IHC) analysis.

2.15 | Protein concentration determination

Protein concentrations were determined using the bicinchoninic acid (BCA) protein assay (Pierce).

2.16 | Quantitative proteomics for plasma Hsp90α detection

2.16.1 | Patients enrolled in quantitative proteomics

Plasma samples were collected from 30 patients with lung cancer who had negative results in ELISA. Diagnosis of patients with lung cancer was confirmed histologically by medical doctors and pathologists. The recruited patients were treatment naïve. Blood samples (EDTA-K2 anticoagulant) from 30 patients were centrifuged at 800 *g* for 10 min. The remained plasma samples were then aliquoted and stored at −80°C, until use.

2.16.2 | Plasma sample preparation

Depletion of high abundance proteins, including immunoglobulin G (IgG) and albumin, from plasma samples was performed using ProteoPrep Blue Albumin and IgG Depletion Kit (Sigma-Aldrich) according to the manufacturer's instructions. Next, a 400 μL aliquot of suspended deletion medium was added to a spin column, and the column centrifuged at 8000 *g* for 5 s to remove the storage solution. Then depletion medium was equilibrated twice with 400 μL equilibration buffer. To discard the equilibration buffer, the spin column was centrifuged at 8000 *g* for 15-30 s. After the equilibration process, 25 μL of plasma sample was applied to the top of the packed medium and incubate at room temperature for 8 min, then the column was centrifuged at 10 000 *g* for 60 s. The elute in the collection tube was transferred to the top medium in the spin column, and incubated at room temperature for another 5 min, and centrifuged as before. The IgG/albumin-depleted plasma samples were stored at −20°C, until use.

2.16.3 | SDS-PAGE and trypsin digestion

Samples mixed with loading buffer were denatured at 95°C for 3 min, and separated on SDS-PAGE gels as previously described. After electrophoresis, gels were stained for 1 h with Coomassie brilliant blue G-250 and destained overnight. Target bands were sliced from the gel, reduced with 10 mmol/L ammonium bicarbonate containing 10 mmol/L DTT, alkylated with 55 mmol/L iodoacetamide, treated with acetonitrile, and then the gel slice was digested with trypsin (Promega) in 50 mmol/L ammonium acetate containing 10% acetonitrile at 37°C overnight.

2.16.4 | Mass spectrometric analysis – parallel reaction monitoring

Parallel reaction monitoring (PRM) analysis was performed using a high-resolution Q Extractive hybrid mass spectrometer coupled with an UltiMate 3000 RSLCnano System (Thermo-Scientific). Briefly, peptides were injected into the UltiMate 3000 RSLCnano System through a reverse phase column silica C18 separate column (300 Å, 5 μm) using an acetonitrile gradient (0%-60% Buffer B in 80 min) at a flow rate of 200 nL/min into a high-resolution Q Extractive hybrid mass spectrometer. The buffer system was: Buffer A, 5% acetonitrile with 0.4% acetic acid and 0.005% heptafluorobutyric acid (HFBA), and Buffer B, 95% acetonitrile 0.4% acetic acid and 0.005% HFBA. The mass spectrometer was operated in an automated data-dependent acquisition mode that was switched between MS scan and HCD-MS using Xcalibur 2.2.0 software. A single full-scan mass spectrum in Orbitrap (300-1800 *m/z*, 70 000 resolution) followed by 20 data-dependent MS/MS scans at 27% normalized collision energy (HCD) were collected.

2.16.5 | Quantitative analysis

The MS/MS spectra from each LC-MS/MS run were searched against human.fasta from UniProt using an in-house Proteome Discoverer program (version PD1.4). The search criteria were as follows: full tryptic specificity was required; two missed cleavages were allowed; carbamidomethyl (C) was set as the fixed modifications; the oxidation (M) was set as the variable modification; precursor ion mass tolerances were set at 20 ppm for all MS acquired in the Orbitrap mass analyzer; and the fragment ion mass tolerance was set at 0.02 Da for all MS2 spectra acquired. The peptide FDR was calculated using Percolator provided by PD1.4. When the *q*

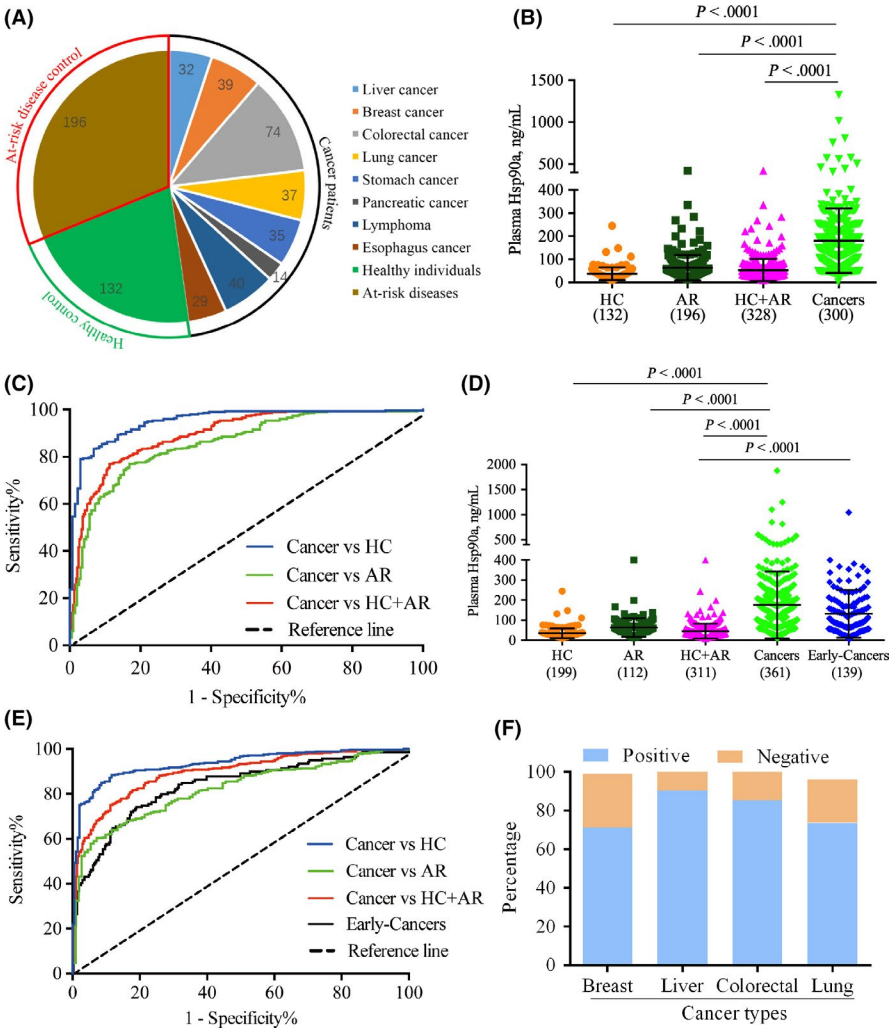

FIGURE 1 Plasma Hsp90α is a diagnosis biomarker for pan-cancer diseases. A, Composition of participants in a test cohort, including healthy individuals, patients with at-risk diseases, and patients with different types of cancer. B, Plasma Hsp90α levels for patients with cancer and different controls in a test cohort. C, ROC curves of plasma Hsp90α for patients with cancer vs different control groups in a test cohort. D, Plasma Hsp90α levels for patients with cancer and different controls in a validation cohort. E, ROC curves of plasma Hsp90α for patients with cancer vs different control groups in a validation cohort. F, The ratio of positive results for plasma Hsp90α in patients with breast cancer, liver cancer, colorectal cancer, and lung cancer. 64.01 ng/mL was used as the cutoff value to calculate the positive ratio of plasma Hsp90α in different types of cancer. HC, healthy control; AR, patients with at-risk diseases, including tuberculosis, benign lung tumor, chronic hepatitis, or mastitis, chronic hepatitis, or colon polyps; Cancers, patients with different types of cancer; Hsp90α, heat shock protein 90alpha

TABLE 1 Diagnostic performance of plasma Hsp90α for detection of cancer malignancy

AUC (95% CI)	Cutoff (ng/mL)	Sensitivity (%)	Specificity (%)	PPV (%)	NPV (%)	Positive LR	Negative LR
Test cohort							
Cancers vs non-cancers							
0.895 (0.870-0.919)	69.19	81.33	81.65	80.26	82.66	4.43	0.23
Cancers vs AR							
0.857 (0.823-0.890)	72.52	80.00	75.90	83.62	71.15	3.32	0.26
Cancers vs HC							
0.951 (0.930-0.972)	54.98	87.00	87.12	93.88	74.67	6.75	0.15
Validation cohort							
Cancers vs non-cancers							
0.893 (0.869-0.917)	64.01	81.72	81.03	83.33	79.25	4.31	0.23
Cancers vs AR							
0.820 (0.781-0.859)	75.10	75.90	71.43	89.54	47.90	2.66	0.34
Cancers vs HC							
0.934 (0.914-0.954)	54.17	87.26	88.94	93.47	79.37	7.89	0.14
Early-cancers vs non-cancers							
0.759 (0.697-0.820)	56.38	76.26	76.53	59.22	87.82	3.25	0.31

Abbreviations: Cancers, patients with different types of cancer; AR, patients with at-risk disease; AUC, area under the curve; CI, confidence interval; Early-cancers indicates patients with multiple early-stage cancer; HC, healthy individuals; LR, likelihood ratio; Non-cancers, including healthy individuals and patients with at-risk disease; NPV, negative predictive value; PPV, positive predictive value

value was <1%, the peptide spectrum match (PSM) was considered to be correct. FDR was determined based on PSMs when searched against the reverse and decoy database. Peptides only assigned to a given protein group were considered as unique. The FDR was also set to 0.01 for protein identifications. From the protein identified results, we chose the unique peptides for quantitative analysis. Skyline software was used to analyze the acquisition data. Quantitation of recombinant Hsp90α (Protgen) was used to draw the standard curve for the concentration calculation of plasma Hsp90α. Criteria for the unique and quantotypic peptide[22] including the peptide with an appropriate peptide length, uniqueness, no miscleavages or modifications, measurable precursor charge, symmetrical and narrow width chromatographic peak, and stable signal intensity, were considered for representative peptide selection.

2.17 | Exosomes isolation

Conditional medium was collected from cell cultures without serum. Exosomes were purified by sequential centrifugation steps. Supernatant fractions were centrifuged at 300 *g* for 10 min, 20 000 *g* for 30 min, and then at 100 000 *g* for 70 min (Beckman). Exosomes pellets were washed again in PBS, and collected by ultracentrifugation at 100 000 *g* for 70 min.

2.18 | Electron microscopy

Exosomes were dropped onto a formvar-carbon-coated grid. The grid was dried at room temperature for 8 min and viewed at ×20 000 and ×50 000 magnification using an electron microscope (Hitachi).

2.19 | Dynamic light scattering (DLS)

The mean hydrodynamic diameters of exosomes and size distribution were estimated by dynamic light scattering (DLS). The light scattering was recorded three times with 30 replicate measurements.

2.20 | Statistical analysis

2.20.1 | Statistical analysis in the diagnosis trial

Data were summarized as mean ± SD. Significance between two independent groups was tested using the non-parametric Wilcoxon Mann-Whitney *U* test. ROC curves were constructed to calculate sensitivity, specificity, and AUCs with 95% confidence interval (CI). The optimum cutoff values were determined according to the Youden index (*J*) method.[23]

2.20.2 | Statistical methods in biochemical research

Experiments were performed in triplicate, and results are shown as mean ± SD. Statistical tests between groups were determined using unpaired Student *t* test using SPSS software (Version 19.0). The chi-squared test was used to test differences between categorical variables for tissue array. A *P*-value < .05 (two sided) was considered to be statistically significant.

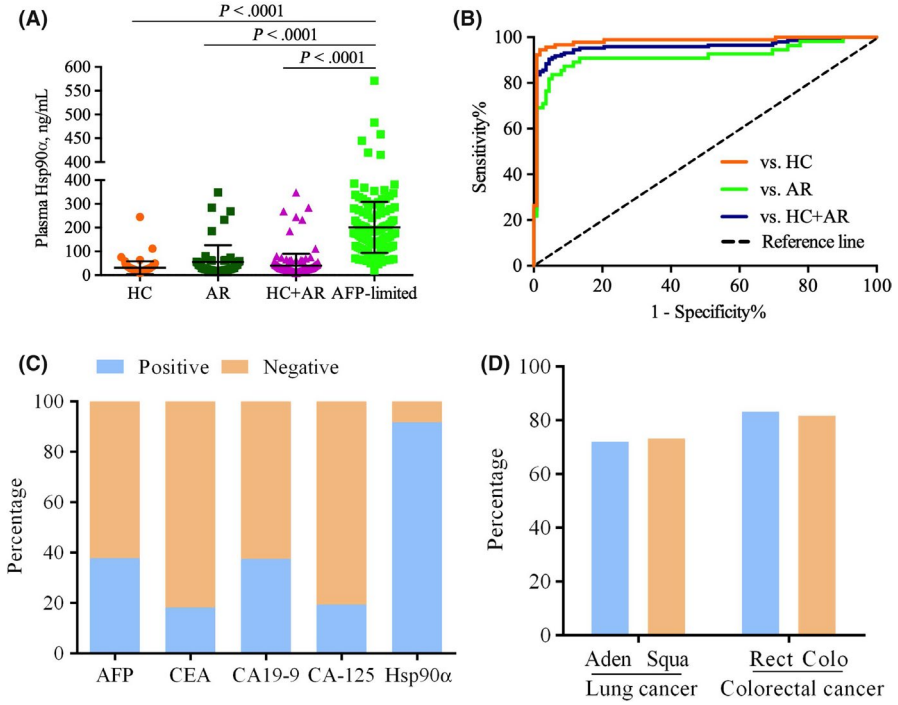

FIGURE 2 Plasma Hsp90α can also be a broad-spectrum biomarker for cancer subtypes. A, Plasma Hsp90α levels for patients with AFP-limited liver cancer and different controls. B, ROC curves of plasma Hsp90α for AFP-limited vs different control groups. C, The ratio of positive results for other different biomarkers, including AFP, CEA, CA19-9, and CA-125, in detecting patients with AFP-limited liver cancer. D, The ratio of positive results for plasma Hsp90α in different subtypes of lung cancer or colorectal cancer. HC, healthy control; AR, patients with at-risk diseases, including tuberculosis, benign lung tumor, chronic hepatitis or mastitis, chronic hepatitis, or colon polyps; AFP, alpha-fetoprotein; CA19-9, carbohydrate antigen 19-9; CA-125, cancer antigen 125; Hsp90α, heat shock protein 90alpha; Aden and Squa means lung adenocarcinoma and squamous cell carcinoma, respectively; Rect and Colo represents rectum and colon cancer, respectively; CA19-9 (37 U/mL), CA-125 (35-65 U/mL), CEA (5 ng/mL), AFP (20 ng/mL) were used as the potential biomarkers for the diagnosis of patients with AFP-limited liver cancer. AFP-limited liver cancer indicates patients with cholangiocarcinoma or combined hepatocellular carcinoma and cholangiocarcinoma

3 | RESULTS

3.1 | Plasma Hsp90α is a novel pan-cancer diagnosis biomarker

To expand the diagnosis potential of plasma Hsp90α for multiple indications, 628 participants, including 300 patients with various cancer types, 196 with common at-risk diseases, and 132 healthy individuals, were prospectively recruited from hospitals into the test cohort (Figure 1A and Supporting Information Figure S1, Tables S1-S3). Plasma Hsp90α concentrations quantified by ELISA were significantly raised in patients with cancer (median 157.80 ng/mL, IQR 87.01-235.50 ng/mL; mean 180.30 ng/mL, SD 139.70) compared with those in the non-cancer control ($P < .0001$; Figure 1B and Table S4) and those in the at-risk control ($P < .0001$; Figure 1B and Table S4). The ROC curve determined the best cutoff value in cancer diagnosis as 69.19 ng/mL compared with the non-cancer control (AUC 0.895, 95% CI 0.870-0.919, sensitivity 81.33%, specificity 81.65%; Figure 1C and Table 1). Similar results were also noted when detecting patients with cancer from the at-risk control (Figure 1C and Table 1).

To confirm the above results from the test cohort, we compiled the validation cohort from our curated clinical data corresponding to lung cancer,[8] breast cancer (to be published), colorectal cancer (to be published), and liver cancer[9] (Figure S1 and Table S5). In the validation cohort, we found that plasma Hsp90α was at significantly different levels between patients with cancer and the non-cancer control ($P < .0001$; Figure 1D and Table S6). The ROC curve showed plasma Hsp90α had AUC 0.893 (95% CI 0.869-0.917, sensitivity 81.72% and specificity 81.03% under the optimum diagnostic cutoff 64.01 ng/mL) in discriminating patients with cancer from the non-cancer control (Figure 1E and Table 1). Similar results were found between patients with cancer and the at-risk group (Figure 1E and Table 1). Plasma Hsp90α concentrations were also increased in patients with early-stage cancers compared with the non-cancer control (Figure 1E and Table S6). In this setting, plasma Hsp90α had an AUC 0.759 (0.697-0.820) with a sensitivity of 76.26% and specificity of 76.53% when using 56.38 ng/mL as the best cutoff value (Figure 1E ad Table 1). Positive ratios in patients with lung cancer, breast cancer, colorectal cancer, or liver cancer, were 73.52%, 71.19%, 85.24%, or 90.25%, respectively (Figure 1F). Collectively, these results proved that plasma Hsp90α is a novel pan-cancer diagnostic biomarker.

3.2 | Plasma Hsp90α can also be a broad-spectrum biomarker for cancer subtypes

While α-fetoprotein (AFP) is a widely used serological biomarker, it could only be applicable for hepatocellular carcinoma (HCC).[24] AFP-limited subtypes, including cholangiocarcinoma or combined hepatocellular carcinoma and cholangiocarcinoma, accounted for the second most common primary liver cancer patients. Due to a lack of a sensitive diagnosis biomarker, the overall survival of these patients was extremely poor.[25] Here we investigated the diagnostic capability of plasma Hsp90α as a broad-spectrum biomarker for cancer subtypes, with an emphasis on patients with liver cancer (Figure S2). In this study, we found that plasma Hsp90α concentrations in AFP-limited liver cancer (median 182.90 ng/mL, IQR 120.60-272.40 ng/mL; mean 201.20 ng/mL; SD 107.40) were significantly elevated compared with the corresponding controls ($P < .0001$; Figure 2A and Table S7). The ROC curve was likewise used to evaluate the diagnosis performance of plasma Hsp90α in this setting. The results showed that the sensitivity of plasma Hsp90α to differentiate patients with AFP-limited liver cancer from the non-cancer control was 91.78% under the cutoff 66.44 ng/mL, and the specificity was 91.96% (Figure 2B and Table S8). Similar results were also shown in comparison with other controls (Figure 2B and Table S8). CA19-9 (37 U/mL), CA-125 (35-65 U/mL), CEA (5 ng/mL), and AFP (20 ng/mL) have been used as potential biomarkers for diagnosis of patients with AFP-limited liver cancer.[25] However, the positive ratio was only 37.86% for AFP, 18.27% for CEA, 37.50% for CA 19-9, and 19.42% for CA-125, in the diagnosis of AFP-limited liver cancer, respectively (Figure 2C). In addition, we found that plasma Hsp90α had almost comparable diagnosis capability in different subtypes of other cancer types, including lung or colorectal cancer (Figure 2D). The above results demonstrated that plasma Hsp90α can also be a broad-spectrum biomarker among different cancer subtypes.

3.3 | Integrative analysis reveals that ADAM10 determines Hsp90α secretion in multiple cancer cell lines

Next, in the clinic, we investigated systematically the diagnosis determinants for plasma Hsp90α. The diagnostic performance was limited to actual situations by many factors. One of these was the upstream regulator involved in its secretion of the biomarker. To screen the factor(s) regulating the secretion of Hsp90α, we analyzed differential expression profiles between normal and tumor tissues from different types of cancer described in a public database (Table S9). Differentially expression genes were overlapped between different types of cancer (Figure S3A). Functional clustering analysis of altered genes revealed a significant enrichment of genes related to the regulation of cell development, response to growth factor, and tissue morphogenesis (Figure S3B). Focusing on the defined pathways regarding extracellular Hsp90α (eHsp90α) function, including extracellular matrix remodeling,[26] angiogenesis,[27] migration and invasion,[28,29] and pathways mediating the secretion of exosomes,[30] genes were specifically chosen for further analysis (Figure 3A). It was hypothesized that, compared with cell lines that secreted low levels of Hsp90α, upregulated genes in high-secretion cell lines could contribute to its secretion. Therefore, the secretion of Hsp90α in different cell lines was first detected quantitatively (Figure 3B). Subsequently, a closer analysis of transcriptome levels between low- and high-secretion cell lines indicated that seven genes were correlated with the secretion of Hsp90α (Figure S3C and Table S10). A small interfering RNA mini-screen identified ADAM10 as the most significant gene based on gene expression data and quantitative results of eHsp90α (Figure 3C and Figure S3D). ADAM10 knockdown consistently decreased the secretion of Hsp90α in other cancer cell lines (Figure 3D). Inhibition of ADAM10 by its inhibitor GI254023X also decreased the secretion of Hsp90α, but not proportionally to that in the knockdown experiment (Figure S3E). Transfection of a plasmid encoding a dominant-negative ADAM10 (ADAM10DN), which will compromise its sheddase function,[31] decreased slightly the secretion of eHsp90α (Figure S3F). To further confirm these findings in vivo, we detected quantitatively Hsp90α secretion in plasma from A375-shADAM10-derived and PANC1-shADAM10-derived xenografts (Figure 3E,F). Ex vivo quantitation revealed significantly decreased levels of plasma Hsp90α in comparison with that from wild-type mice (Figure 3G). These data determined that ADAM10 regulate the secretion of eHsp90α both in in vitro and in vivo models.

3.4 | ADAM10 is highly expressed in multiple cancers and correlated with levels of plasma Hsp90α

Previous reports have indicated that ADAM10 is overexpressed in several cancer types.[32,33] In addition, levels of plasma Hsp90α were correlated with tumor malignancy in pan-cancer cases (Figure 4A). Accordingly, we hypothesized that ADAM10 would be correlated with tumor malignancy in other major cancer types. To confirm this, we first examined protein levels of ADAM10 using immunohistochemistry in tissue microarray that contained five major epithelial carcinoma tissues, including breast, lung, prostate, colon, and rectum (Table S11). Tissues were scored according to staining intensities of ADAM10 expression and the percentage area of cancer cells. It was shown that expression of ADAM10 was significantly elevated in tissues from patients with cancer compared with those from normal controls (Figure 4B,C). Also, we found that the expression of ADAM10 in patients with late-stage diseases was significantly elevated compared with that in early-stage patients (Figure 4C and Figure S4A), which indicated that ADAM10 played a critical role in tumor progression.

To further establish in the clinic, the correlation between ADAM10 and the secretion of Hsp90α, we detected the expression of ADAM10 from patients with lung or colorectal cancer, in which

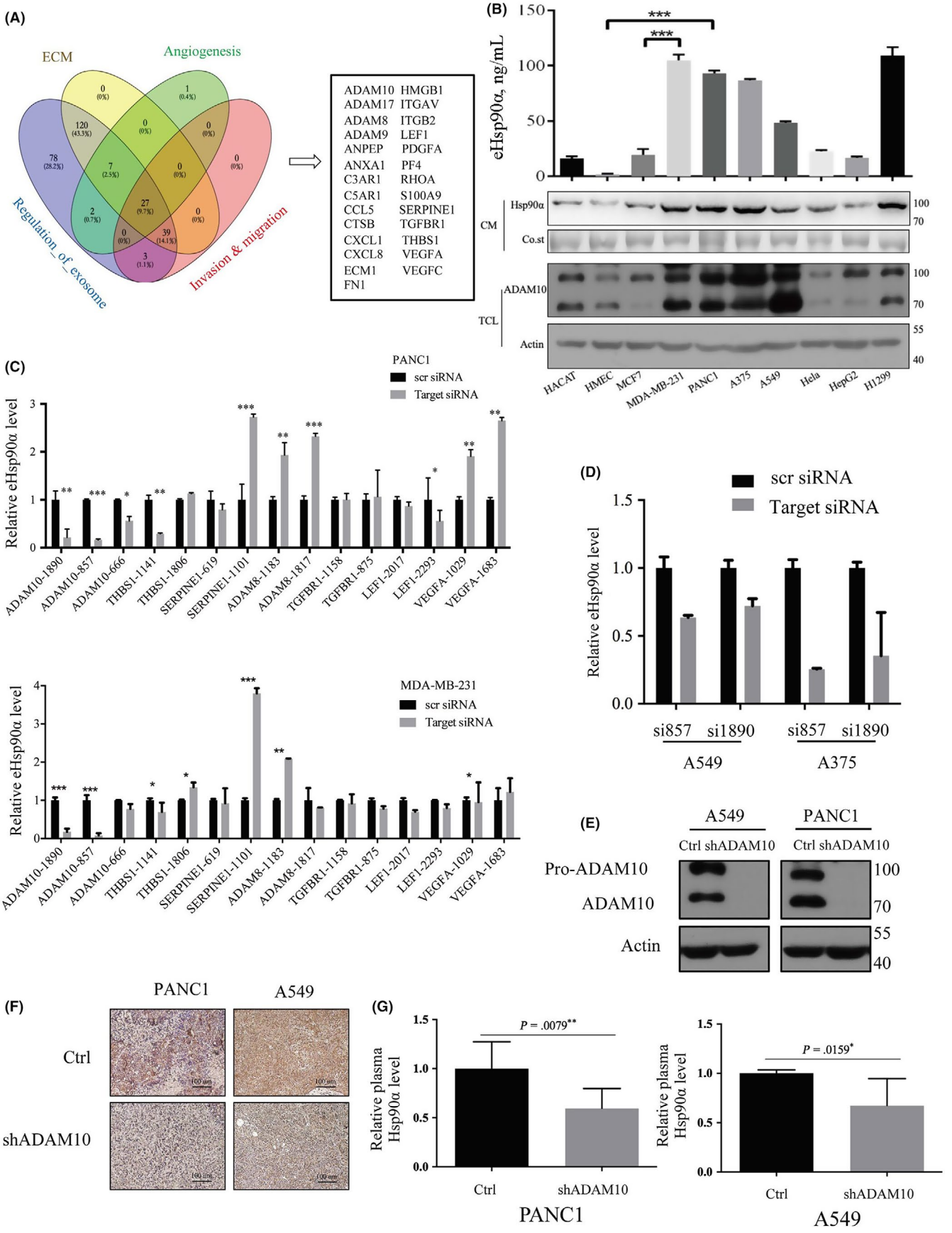
(A)
ECM
Angiogenesis
Regulation_of_exosome
Invasion & migration
0 (0%)
1 (0.4%)
120 (43.3%)
0 (0%)
0 (0%)
78 (28.2%)
7 (2.5%)
0 (0%)
0 (0%)
2 (0.7%)
27 (9.7%)
0 (0%)
0 (0%)
39 (14.1%)
3 (1.1%)
ADAM10 HMGB1
ADAM17 ITGAV
ADAM8 ITGB2
ADAM9 LEF1
ANPEP PDGFA
ANXA1 PF4
C3AR1 RHOA
C5AR1 S100A9
CCL5 SERPINE1
CTSB TGFBR1
CXCL1 THBS1
CXCL8 VEGFA
ECM1 VEGFC
FN1
(B)
eHsp90α, ng/mL
150
100
50
0
***
***
CM
Hsp90α
Co.st
TCL
ADAM10
Actin
100
70
100
70
55
40
HACAT
HMEC
MCF7
MDA-MB-231
PANC1
A375
A549
Hela
HepG2
H1299
(C)
PANC1
scr siRNA
Target siRNA
Relative eHsp90α level
ADAM10-1890
ADAM10-857
ADAM10-666
THBS1-1141
THBS1-1806
SERPINE1-619
SERPINE1-1101
ADAM8-1183
ADAM8-1817
TGFBR1-1158
TGFBR1-875
LEF1-2017
LEF1-2293
VEGFA-1029
VEGFA-1683
MDA-MB-231
scr siRNA
Target siRNA
Relative eHsp90α level
(D)
scr siRNA
Target siRNA
Relative eHsp90α level
si857
si1890
si857
si1890
A549
A375
(E)
A549
PANC1
Ctrl shADAM10
Ctrl shADAM10
Pro-ADAM10
ADAM10
Actin
100
70
55
40
(F)
PANC1
A549
Ctrl
shADAM10
100 um
(G)
P = .0079**
Relative plasma Hsp90α level
Ctrl
shADAM10
PANC1
P = .0159*
Relative plasma Hsp90α level
Ctrl
shADAM10
A549

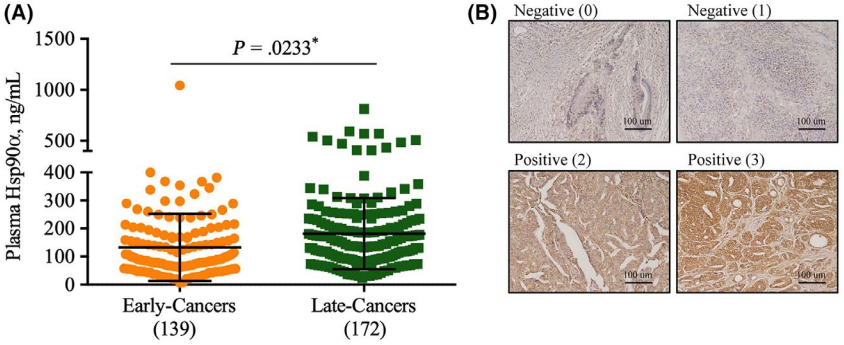

(C)

Variable	Score 0	Score 1	Score 2	Score 3	Chi-square test
Total population					<0.0001***
Normal	4	9	3	0	
Malignant	12	31	75	71	
Stage					
I	5	11	26	6	0.0023**
II	5	15	28	46	
III-IV	2	5	21	19	
Grade					0.0226*
1	7	9	14	12	
2	4	15	39	43	
3	0	3	14	7	

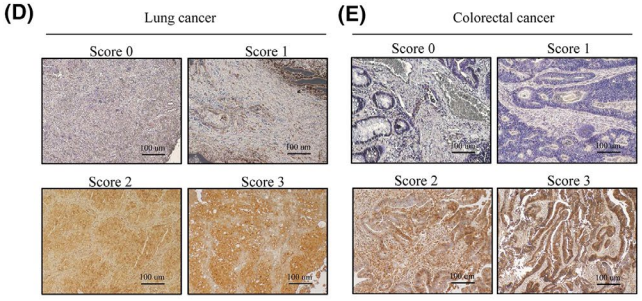

(F)

Variable	Lung cancer			Colorectal cancer		
	Low	High	0.0455*	Low	High	0.0201*
Score 0+1	4	8		8	7	
Score 2+3	1	17		2	13	

FIGURE 4 ADAM10 is highly expressed in multiple cancers and correlated with levels of plasma Hsp90α. A, Levels of plasma Hsp90α were correlated with tumor malignancy in pan-cancer cases. Early-Cancers, patients with early-stage cancers. Late-Cancers, patients with late-stage cancers. B, Representative images of ADAM10 staining in normal tissues and malignant samples which illustrate immunohistochemical scores of 0, 1, 2, and 3. Scale bar, 100 μm. C, Association of ADAM10 immunohistochemical scores with tumor malignancy (I, II, III + IV) and tumor grade (1, 2, 3). The chi-squared test was used to test the difference between categorical variables. D, E, Representative images of ADAM10 expression in 30 patients with lung cancer (D) or colorectal cancer (E), in which levels of plasma Hsp90α were quantified with the ELISA kit. Scale bar, 100 μm. F, Associations of ADAM10 immunohistochemical scores with the secretion of plasma Hsp90α. The chi-squared test was used to test difference between categorical variables. Cutoff value of plasma Hsp90α for cancer diagnosis was 69.19 ng/mL

corresponding levels of plasma Hsp90α from the same patients were quantified by the ELISA kit. The results showed that high expression of ADAM10 was correlated with the levels of plasma Hsp90α in both cancer types (Figure 4D-F). The above results proved that ADAM10 was correlated with the secretion of Hsp90α in patients and will determine diagnostic performance of biomarker plasma Hsp90α.

FIGURE 3 Integrative analysis reveals that ADAM10 determines the secretion of the biomarker Hsp90α in multiple cancer cell lines. A, Twenty-seven genes related with four defined signaling pathways related with extracellular Hsp90α, including extracellular matrix remodeling, angiogenesis, invasion and migration, and pathways in regulation of exosome secretion. B, Levels of secreted Hsp90α and the expression of ADAM10 from multiple cell lines. The secreted Hsp90α was detected quantitatively with the ELISA kit and by western blotting with a well established anti-Hsp90α antibody. CM indicates conditional medium; TCL means total cell lysates; Co.st represents Coomassie blue staining. C, A small interfering RNA mini-screen identified ADAM10 as the most significant gene in the regulation of Hsp90α secretion in MDA-MB-231 and PANC1 cell lines. Data are expressed as the secretion of extracellular Hsp90α compared with the control scramble RNA. scr siRNA indicates scramble siRNA. D, Knockdown of ADAM10 can also decrease the secretion of Hsp90α in other cancer cell lines. Data are expressed as the secretion of extracellular Hsp90α compared with the control scramble RNA. si857 and si1890 are two different siRNA against ADAM10. scr siRNA indicates scramble siRNA. E, ADAM10 expression in stably knockdown tumor cell lines. F, Representative images of immunohistochemical staining of ADAM10 in tumor sections derived from PANC1- or A549-derived tumor xenografts. Scale bar, 100 μm. G, Ex vivo quantitation of plasma Hsp90α from PANC1-derived (left) or A549-derived (right) xenografts in comparison with that from wild type mice. Data are represented as mean ± SD. *P < .05; **P < .01; ***P < .001

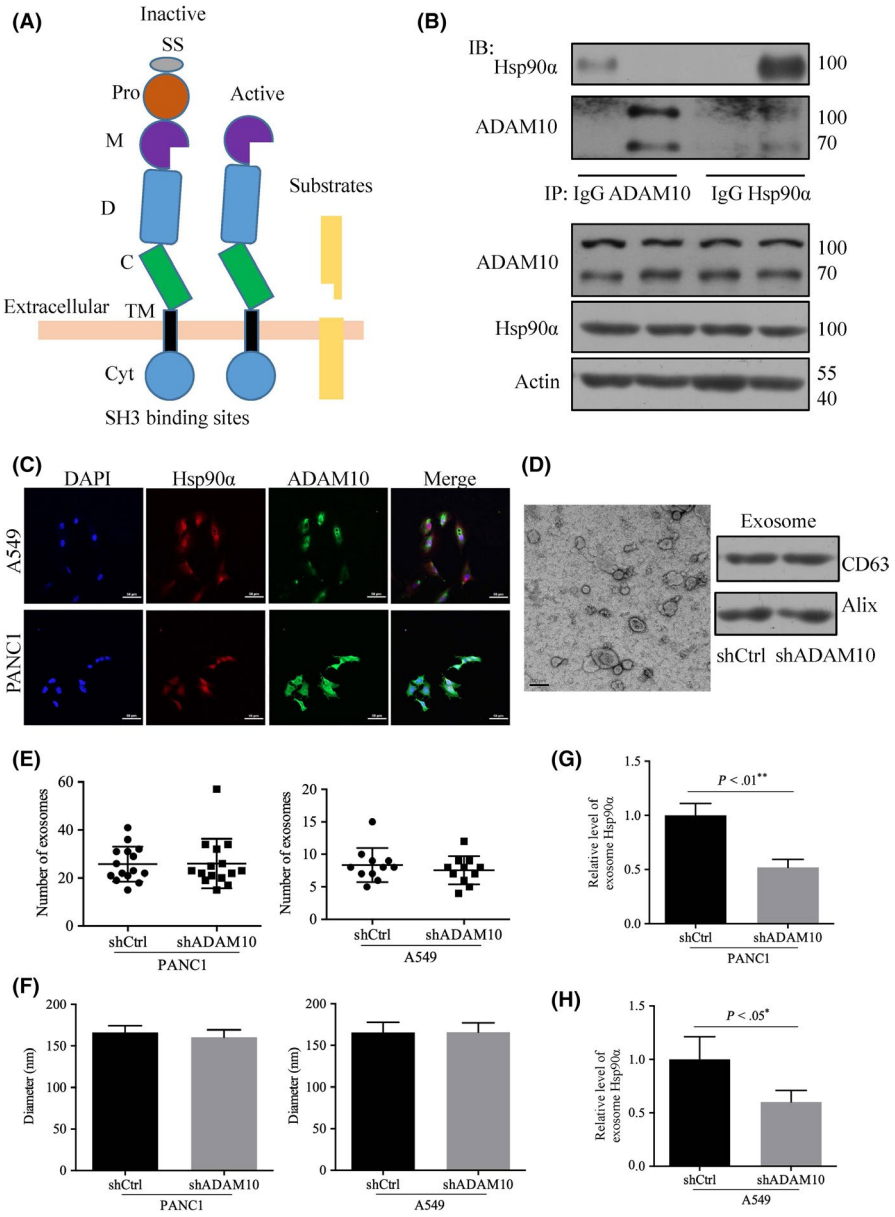

FIGURE 5 ADAM10 affects the content of Hsp90α in exosomes, not the classical direct sheddase function. A, Schematic diagram of ADAM10 protein. C, cysteine-rich; Cyt, cytoplasmic tail; D, disintegrin; M, metalloproteinase; Pro, prodomain; SS, signal sequence; TM, transmembrane. B, Lysates of PANC1 cells were subjected to immunoprecipitation (IP) with an anti-Hsp90α antibody (IP: Hsp90α), a control IgG (IgG) and an anti- Hsp90α antibody. The immunoprecipitates were resolved by SDS/PAGE and immunoblotted with the respective antibodies. C, Colocalization of Hsp90α and ADAM10. PANC1 or A549 cells were cultured in coverslips. ADAM10 were stained with tetramethylrhodamine isothiocyanate (TRITC)-phalloidin (red) and nuclei were stained with 4′,6-diamidino-2-phenylindole (DAPI) (blue). Hsp90α was stained with fluorescein isothiocyanate (FITC) (green). Scale bar: 50 μm. D, Isolation of exosomes from wild type and knockdown groups. Exosomes were isolated by sequential centrifugations from conditional medium. Scale bar, 100 nm. An inset panel shows the exosome marker, tetraspanin protein CD63 and Alix by western blot. E, Quantitation of exosome number. F, The size distribution of exosomes was analyzed by DLS, and given as average ± standard deviation. G, H, Levels of secreted Hsp90α in isolated exosomes were detected by ELISA assay when the PANC1 (G) and A549 (H) cells were transfected with different plasmids

3.5 | ADAM10 affects the content of Hsp90α in exosomes, not the classical direct sheddase function

The mechanism underlying ADAM10 that regulates the secretion of Hsp90α is unknown. ADAM10, a single-pass transmembrane protein with multiple organized modular domains (Figure 5A), is well known as the major sheddase in physiological process.[34] In the ADAM family of sheddase, several other proteolytic members closely related to ADAM10 were also overexpressed in human cancers (Figure S5A). To confirm the findings that ADAM10, rather than other A Disintegration And Metalloproteinase domain-containing proteins (ADAMs), regulates the secretion of Hsp90α, we used an RNA

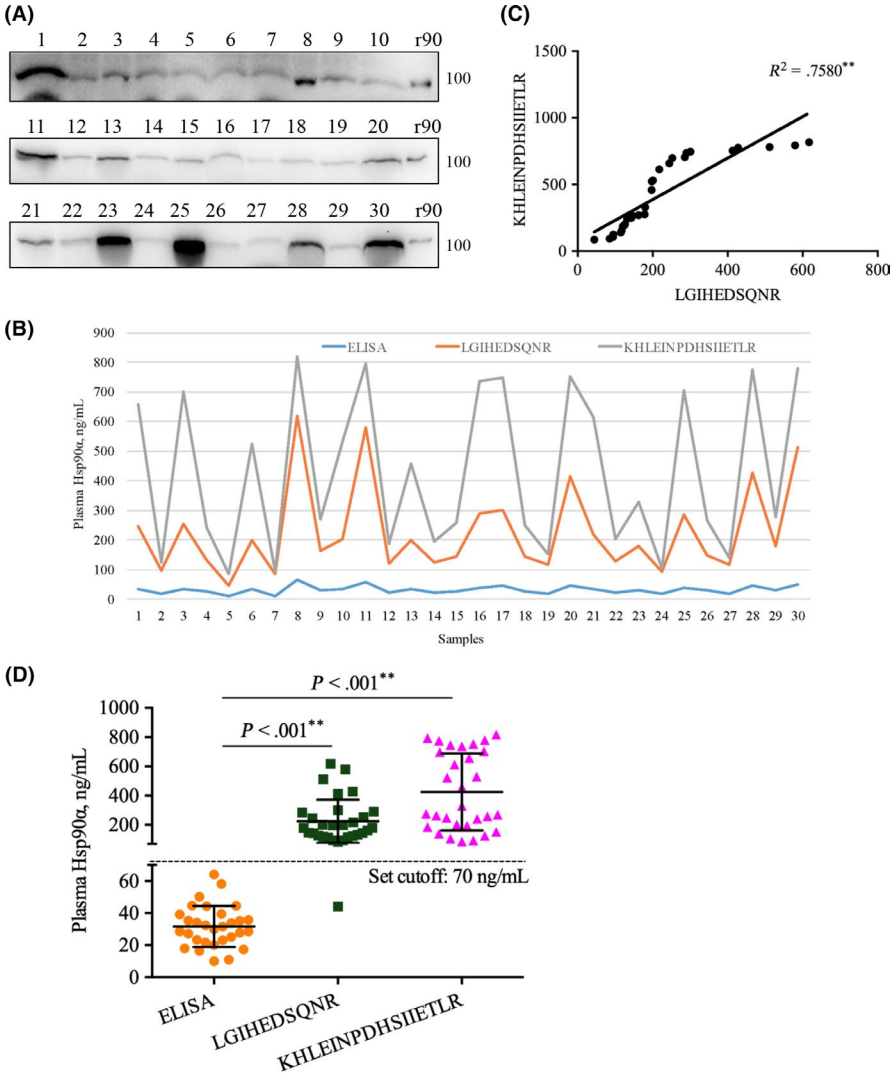

FIGURE 6 Western blotting and quantitative proteomic method determined high levels of plasma Hsp90α from partial false ELISA-negative patients. A, Detection by western blotting of plasma Hsp90α from ELISA-negative lung patients with cancer. r90, recombinant Hsp90α (70 ng/mL). B, PRM quantitation of plasma Hsp90α from false ELISA-negative patients. C, Plasma Hsp90α concentration profiles categorized in false ELISA-negative patients with cancer: PRM vs ELISA. PRM detected always a higher concentration of plasma Hsp90α in these patients with cancer. D, Correlation of plasma Hsp90α concentration using two different representative peptides: LGIHEDSQNR and KHLEINPDHSIIETLR

knockdown approach. Studies were conducted in two cell lines with high-secretion levels of Hsp90α (PANC1 and A549). Knockdown of other ADAMs did not decrease significantly the secretion of eHsp90α (Figure S5B-E). ADAM10 is comprised of a proform of *c*. 100 kDa and mature form of *c*. 68 kDa.[35] To be able to perform functional experiments to address the causative roles of ADAM10 in the secretion of Hsp90α, subsequent experiments were conducted in cell lines with high secretion of eHsp90α and high expression of ADAM10 (Figures 3B and S5F). As the secreted form of Hsp90α is cleaved,[36] therefore we firstly assessed whether Hsp90α could be one of the substrates of ADAM10. The interaction between ADAM10 and Hsp90α was investigated in PANC1 and A549 cell lines. However, co-immunoprecipitation (co-IP) results showed no direct interaction between ADAM10 and Hsp90α (Figure 5B). Next, we detected the subcellular localization of ADAM10 and Hsp90α. Confocal fluorescence microscopy showed that ADAM10 and Hsp90α did not colocalize (Figure 5C). The secretion of Hsp90α was reported to be through the exosome pathway.[30] Therefore, we detected the effect of ADAM10 on exosomes. It was found that knockdown of ADAM10 decreased the eHsp90α content in exosomes, but not the size or the number of exosomes (Figure 5D-H). In summary, ADAM10 regulated Hsp90α secretion by affecting its content in exosomes, not by the classical direct sheddase function.

3.6 | Western blotting and quantitative proteomic methods determine high levels of plasma Hsp90α from partial false ELSIA-negative patients

Different glycoforms of AFP, AFP-L1 to AFP-L3 have been identified in the serum of HCC patients.[37] In addition, Chiosis's group reported that multiple Hsp90 species existed in cancer cells.[38] All these finding promoted us to test whether secreted Hsp90α was also heterogeneous, as this could contribute to the diagnosis uncertainties of plasma Hsp90α. Prior to validation of above hypothesis, we determined the absolute concentration of plasma Hsp90α from ELISA-negative patients with cancer. Considering that the antibody in the quantitative ELISA kit recognized only the native conformation of antigen, therefore we first used western blotting with a well characterized polyclonal antibody[39] to detect the denatured plasma Hsp90α from ELISA-negative patients. It was found that, in some

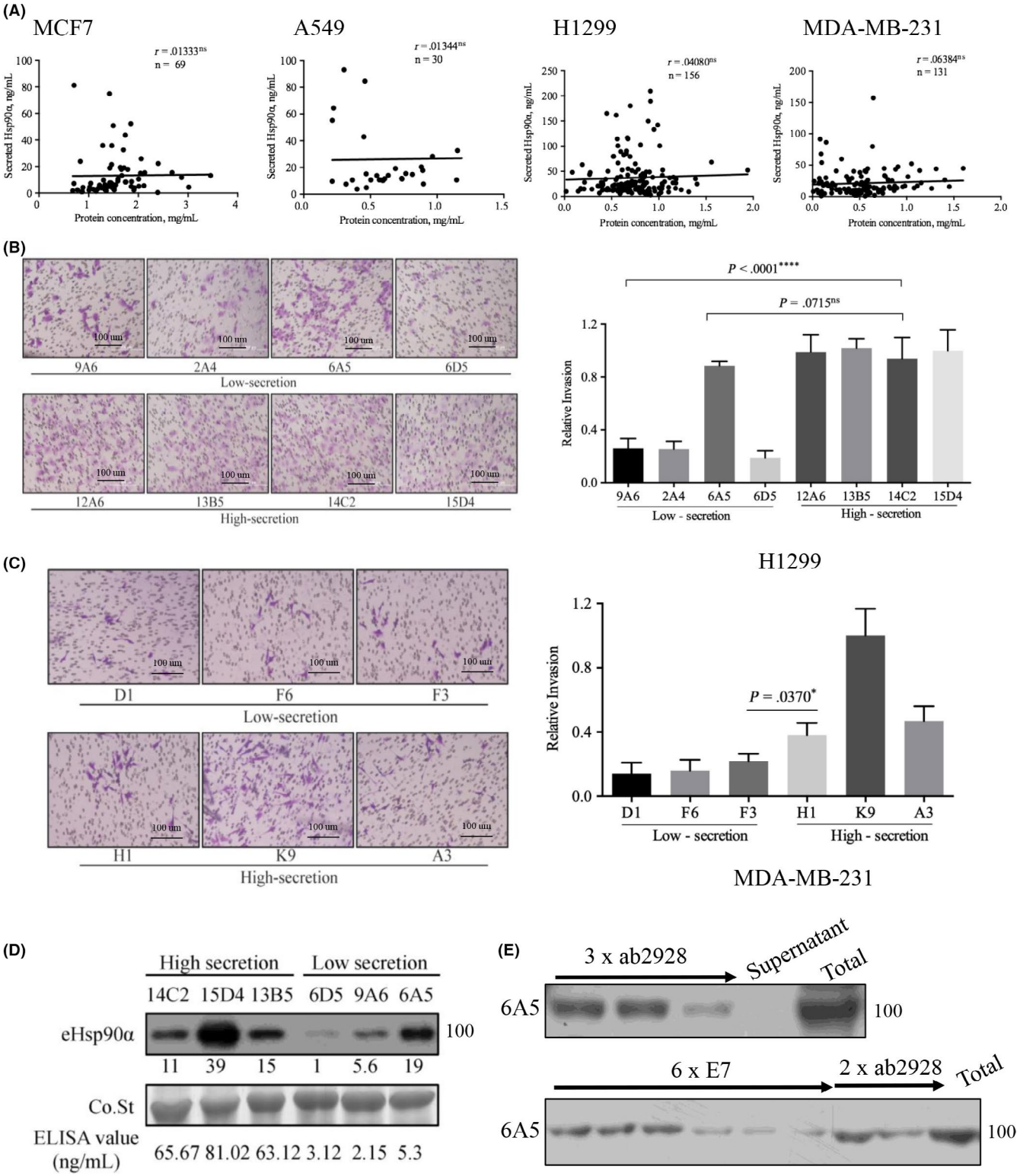

FIGURE 7 Development of cell line model that could recapitulate the antigen recognition heterogeneity. A, Correlation analysis between secreted Hsp90α and subclone proliferation from different cell lines. Extracellular Hsp90α was quantified using the ELISA kit. Total protein concentration was determined with BCA assay. B, C, Comparison of invasion ability between subclones with low and high secretion of eHsp90α from H1299 cells (B) and MDA-MB-231 cells (C). Different subclones were seeded on Matrigel-coated transwell inserts in the invasion assay. Representative images and quantification results of invasion assays by H1299 cells (Scale bar, 100 μm) or MDA-MB-231 cells (Scale bar, 100 μm) are shown. $^{**}P < .01$, $^{***}P < .001$. D, Immunoblot detecting the levels of eHsp90α from different subclones. E, Sequential immunoprecipitation steps with indicated antibodies quantitatively depleted Hsp90α from the conditioned medium from corresponding subclones. E7, the antibody in the ELISA kit; ab2928, a well-characterized Hsp90α polyclonal antibody; Total, total Hsp90α in immunoprecipitation assay detected with ab2928

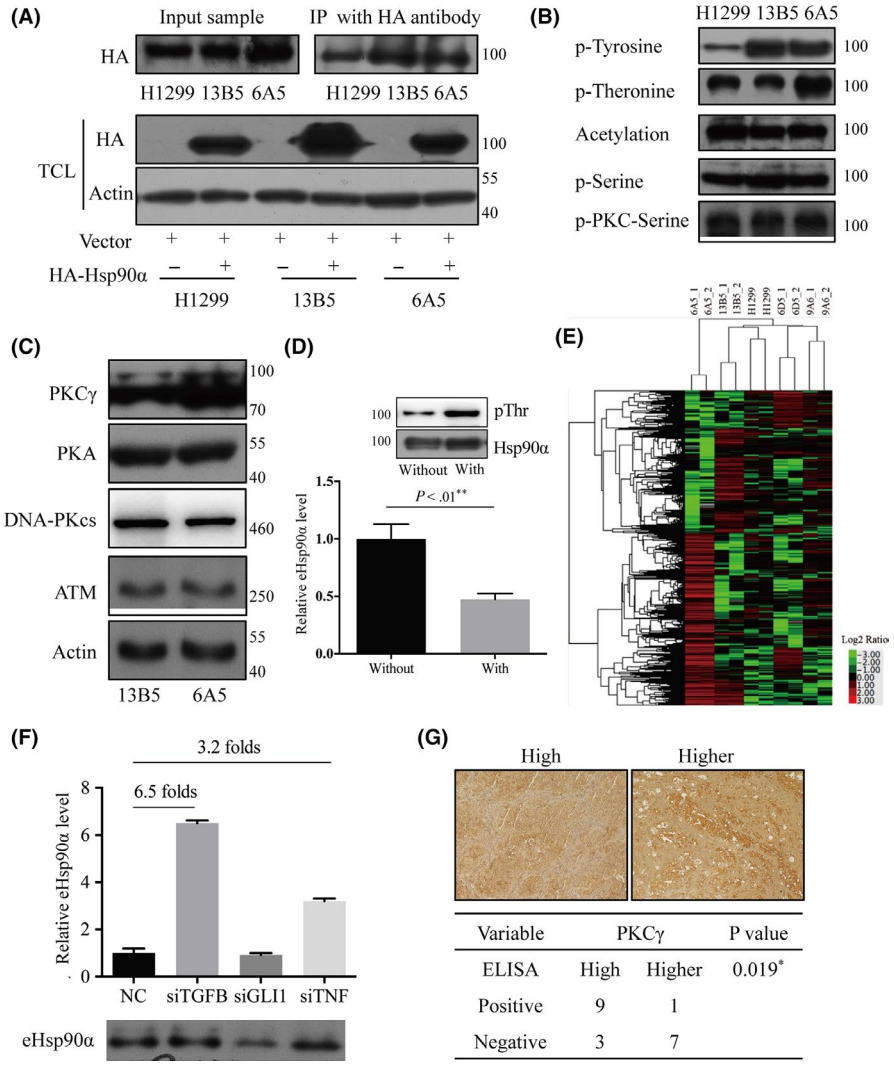

Variable	PKCγ		P value
ELISA	High	Higher	0.019*
Positive	9	1	
Negative	3	7	

FIGURE 8 Secreted Hsp90α hyperphosphorylated by PKCγ confers its antigen heterogeneity. A, Lysates of different subclones transfected with control (Vector) or HA-tagged Hsp90α-expressing vectors were subjected to immunoprecipitation with an anti-HA antibody (IP: HA antibody). The lysates and immunoprecipitates were resolved by SDS/PAGE and immunoblotted with the respective antibodies. B, The immunoprecipitates were probed with the indicated antibodies against corresponding post-translational modifications of secreted Hsp90α. C, Lysates of subclone 6A5 were subjected to detect PKCγ, ATM, DNA-PKcs, and PKA, by which could phosphorylate eHsp90α. D, In vitro phosphorylation of recombinant Hsp90α by PKCγ (inset) and ELISA quantification of the phosphorylated recombinant Hsp90α. E, Heat map of RNA-seq data, which demonstrates similarity in global gene expression between different subclones, including 6A5, low-secretion subclones 6D6 and 9A6, high-secretion subclones 13B5, and wild type H1299 cell line. F, Quantitation of eHsp90α from subclone 6A5 after knockdown of TGFB1, GLI1, and TNF. The bottom panel means the secreted Hsp90α detected by western blotting with ab2928. These three TFs were predicted by IPA analysis to regulate the downstream gene expression leading to the heterogeneity of eHsp90α. G, Immunohistochemical analysis of PKCγ in 10 ELISA-positive patients and 10 false ELISA-negative patients with lung cancer. Samples were divided into two groups, high and higher group, according to the expression of PKCγ; 10 ELISA-positive patients were from Figure 4F, and false ELISA-negative patients were from Figure 6A. Fisher's exact test was used to test the difference between categorical variables. Scale bar, 100 μm

false ELISA-negative patients, western blotting detected higher levels of secreted plasma Hsp90α than the cutoff value (Figure 6A).

In earlier studies, a quantitative proteomic method was used to quantify other biomarkers, including 14-3-3 protein, gelsolin, leptin, and prostate specific antigen (PSA).[40,41] In this approach, a PRM-based targeted proteomic platform was used to detect actual concentrations of plasma Hsp90α, especially in ELISA-negative patients. Two peptides, LGIHEDSQNR and KHLEINPDHSIIETLR, were chosen as the signature peptides, and standard curves were drawn to quantify the concentrations of plasma Hsp90α (Figure S6A,B). Analysis of two representative peptide quantifications revealed that different peptides from same protein showed different absolute concentration measurements in determining the concentration of plasma Hsp90α (Figure 6B). However, quantitative results from LGIHEDSQNR and KHLEINPDHSIIETLR correlated (Figure 6C), although the average difference in quantification measurements was

1.89-fold. We also found that, in false ELISA-negative patients, the mean of plasma Hsp90α quantified by PRM proteomics was significantly higher than that quantified by ELISA (7.09-fold for LGIHEDSQNR and 13.42-fold for KHLEINPDHSIIETLR; Figure 6D and Table S12). The above results showed that plasma Hsp90α from partial response patients with cancer was heterogeneous, could not be detected by the ELISA kit, and affected the diagnosis performance of the ELISA kit.

3.7 | Development of a cell subclone model recapitulates the plasma Hsp90α recognition heterogeneity in clinic

Considering that tumor heterogeneity confers a unique identity on individual cancer cells,[42] it was hypothesized that the heterogeneity above could be recapitulated by different subclones populated from single cells. We first expanded single tumor cells from different cancer cell lines (Figure S7A), and then validated the feasibility that different subclones recapitulated the properties of secreted Hsp90α, including not being related to cancer cell proliferation,[36] but to pro-migration/pro-invasion.[43] We used the BCA assay to quantify protein content and an ELISA kit to detect the secreted Hsp90α from clonally expanded subclones in MCF7, A549, H1299, and MDA-MB-231 clones. There was no significant correlation between the rates of proliferation and secretion of Hsp90α (Figure 7A). We also used the 3-(4,5-dimethylthiazol-2-yl)-2,5-diphenyltetrazolium bromide (MTT) assay to compare the proliferation rates between high-secretion and low-secretion single clones, and no difference was noticed in different groups (Figure S7B-D). Next, we investigated whether subclones sorted by levels of Hsp90α secretion could reflect the invasion difference. Invasion assays were performed using different subclones from H1299 and MDA-MB-231. Compared with the high-secretion group, decreased invasion cell numbers were observed in the low-secretion group in subclones from both H1299 and MDA-MB-231 clones (Figures 7B,C and S7E).

Unexpectedly, one subclone from H1299, 6A5, showed a comparable invasion ability with subclones from the high-secretion group (Figure 7B). We hypothesized that eHsp90α from 6A5 was not recognized by the antibody in the ELISA kit, and classified erroneously into low-secretion group. Therefore, we used western blotting analysis to detect denatured eHsp90α from different subclones. The results showed that the level of eHsp90α from 6A5 was comparable with that from the high-secretion subclones (Figure 7D), which suggested that the partial antigen was not originally recognized by the antibody in the kit during the subclone sorting process. To further confirm this conclusion, consecutive immunoprecipitation (IP) assay was performed to recapitulate the heterogeneous eHsp90α from subclone 6A5. Three IP steps with the mentioned characterized polyclonal antibodies for Hsp90α[44] quantitatively depleted eHsp90α (Figure 7E). In contrast, sequential pull-downs with the antibody in the ELISA kit removed only a limited fraction of eHsp90α from subclone 6A5 (Figure 7E). All these results proved that subclones expanded from single cell can recapitulate the properties of eHsp90α and reflect the heterogeneity in antigen recognition.

3.8 | Hsp90α hyperphosphorylated by PKCγ confers antigen heterogeneity

Having established an in vitro cell model capable of heterogeneous antigen profiling, we next investigated the underlying mechanisms. It was reported that secreted Hsp90α can be phosphorylated[36] and acetylated.[44] Therefore, one plausible explanation for the above phenomenon would be specific post-translational modification of antigen affecting the binding affinity in epitope recognition by the monoclonal antibody in the ELISA kit. To test this hypothesis, HA-tagged Hsp90α plasmids were transfected into wild-type H1299 cells, 6A5, and 13B5, respectively (Figure 8A). After conditioned medium was collected and immunoprecipitated with anti-HA antibody, the immunoprecipitates were then analyzed by western blotting with antibodies against specific post-translational modifications. It was found that acetylation of eHsp90α was comparable in different subclones (Figure 8B). Notably, eHsp90α from subclone 6A5 was hyperphosphorylated at threonine residues compared with that in other subclones (Figure 8B). It has been reported that threonine residues of Hsp90α in human cells can be phosphorylated by PKCγ,[20] ATM,[45] DNA-PKcs,[46] and protein kinase A (PKA).[47] Therefore, we detected these four proteins in subclone 6A5, and found that the expression of PKCγ was elevated (Figure 8C). The in vitro phosphorylation of recombinant Hsp90α by PKCγ also decreased the detection capability of the ELISA kit (Figure 8D).

We next performed mRNA sequencing (mRNA-seq) to compare the global gene expression profiles of different subclones with heterogeneous antigen to view the transcriptional changes. As determined, differential gene expression was significantly different from that in the parental cell line, low-secretion, or high-secretion subclones (Figure 8E). Compared with the high-secretion subclone 13B5, 1183 genes were upregulated at the transcriptome level (Figure S8A). To understand the molecular mechanisms leading to the heterogeneity of eHsp90α, GSEA analysis was performed in upregulated differentially expression genes. The results showed that 78 gene signatures were significantly enriched (FDR < 0.25, $P < .01$; Table S13). Next, using IPA analysis, we identified the upstream transcriptional regulators that could most probably explain the heterogeneity of eHsp90α in 6A5, and three transcription factors, including T-cell growth factor beta 1 (TGFB1), GLI1, and tumor necrosis factor (TNF), were chosen for further analysis. To validate the results of the IPA analysis, we knocked down these three TFs in subclone 6A5 and found that the ELISA kit could detect more eHsp90α from subclone 6A5 when TGFB1 was knocked down (Figures 8F and S8B). In the clinic, we also found that the expression of PKCγ in false ELSIA-negative patients was higher than that in ELISA-positive patients (Figure 8G). All these results indicated that TGFB1-PKCγ defines a distinct pool of eHsp90α hyperphosphorylated at threonine residues that can affect the diagnostic performance of plasma Hsp90α in the clinic.

4 | DISCUSSION

Here we have presented an ELISA-based quantitation of protein biomarker plasma Hsp90α as an early, convenient, accurate, and fast (e-CAF) liquid biopsy method for pan-cancer diagnosis, particularly for patients with early-stage cancer. Plasma Hsp90α can discriminate more than 81% of patients with cancer from healthy individuals and from patients with at-risk diseases, and maintained a 76% accuracy in detecting patients with different early-stage cancers. In addition, using plasma Hsp90α as a model system, both the upstream regulator ADAM10 affecting its secretion and antigen heterogeneity of Hsp90α determined its diagnostic performance as a pan-cancer biomarker; this provided fundamental implications for understanding its use in the clinic.

Molecular chaperones, especially Hsp90, are evolutionarily conserved classes of proteins that assist normal folding, intracellular protein disposition, and proteolytic turnover of the key regulators of cell growth. However, in cancer cells, the Hsp90 transient and multi-protein complexes are subverted to stabilize activated and metastable oncoproteins, and buffer cellular stress induced by malignant transformation.[48] Hsp90 accounts for 1%-2% of cellular proteins in normal cells, but 2%-7% in cancer cells.[49] Recently, it has been reported that Hsp90α can be secreted from many cancers, including skin, breast, colon, bladder, prostate, ovary, liver, and bone.[5] Extracellular Hsp90α is also involved is multiple physiological and pathological signaling pathways.[50] Researchers have reported that metastasis at the molecular level occurred in the early stage of cancer progression, and provided evidence supporting detection for early-stage cancer.[51,52] Therefore, the central position occupied by functional intracellular or extracellular Hsp90α in maintaining cancer hallmarks[53,54] has demonstrated the feasibility of plasma Hsp90α as a novel pan-cancer diagnosis biomarker. The levels of secreted plasma Hsp90α are gradually increased from healthy individuals, through to patients with at-risk diseases, to patients with different types of cancer, suggesting that an increase in Hsp90α secretion is an early event in the multistep progress of cancer carcinogenesis. Given that the etiology is different between the East and the West, the diagnostic performance of plasma Hsp90α in Western populations still needs further investigation.

The investigation of diagnosis determinants makes it possible to address causes and anticipated risks of outlier samples judged by tumor biomarkers in the clinic, such as patients with cancer identified erroneously as healthy individuals. In the present study, we found that ADAM10 could regulate the secretion of Hsp90α by affecting its content in exosomes. ADAM10 has been identified consistently to be the most relevant and physiological enzyme in the RIPing and shedding of many substrates that drive cancer malignancy.[33] Proteolytic shedding of membrane protein is increasingly reported to be an important post-translational modification that promotes cancer progression. Metalloproteinase domain-containing proteins (ADAM family) have been implicated to catalyze many cell surface endoproteolytic events, including Notch, E-cadherin, epidermal growth factor (EGF), ErbB2, CX3CL-1, IL-6 receptor, CD44, CD23, and L1.[34] Therefore, it is possible that these cytokines or signaling molecules mediate indirectly the secretion of Hsp90α in the regulation of ADAM10. Emerging studies have also reported that ADAM10 is required for CD23 or L1 sorting into exosomes.[55,56] The exact mechanism underlying ADAM10 in mediating the secretion of Hsp90α needs further studies. We also examined the signaling pathways in regulating the secretion of Hsp90α after dysregulating the expression of ADAM10. No consistent conclusions could be drawn from multiple cancer cell lines (data not shown). Furthermore, many other factors, including FKBP52, PKA, PP5, CHIP, Cyp40,[36] HIF1α,[49] and HDAC6,[44] have been reported to be involved in the secretion of Hsp90α. Consequently, the relationships between these factors and ADAM10 also need further investigation.

Western blotting and proteomic methods tend to measure the actual total concentration in a denatured setting. However, the ELISA kit quantifies the target proteins through an epitope exposed in solution. In addition, the interaction between target antigen and antibody in a kit can also be affected by autoantibodies, other bound proteins, or even post-translational modifications (PTM). In our study, it was found that threonine residues in plasma Hsp90α hyperphosphorylated by PKCγ affected the diagnostic capability of the ELISA kit. PKC, known as a family of serine/threonine kinases, contributes to several cancer progressions including tumor migration and invasion.[57] The γ isoform has been shown to be a substrate of Hsp90, and Hsp90α can be phosphorylated by PKCγ.[20] However, the mechanisms underlying PKCγ hyperphosphorylated Hsp90α in those specific population still are not known. The glycoform AFP-L3,[37] but not L1 or L2, is the marker for hepatocellular carcinoma. Wu and coworkers[58] have reported that N-glycan heterogeneity of α1-acid glycoprotein (AGP) and haptoglobin (Hp) will regulate the interactions of plasma proteins. Meanwhile, it has been reported that phosphorylation of Hsp90 can affect its interaction with co-chaperones or client proteins.[59,60] However, limited by current techniques, the detection of specific sites modified in plasma Hsp90α failed in our study. It is possible that knowledge of the defined spatial position of residues with PTMs and how these PTMs control structure conformation in extracellular Hsp90α is critical for its quantification. All these detailed mechanism studies provide a rational interpretation for its use as a diagnostic biomarker in the clinic, and will ultimately lead to a way to improve the diagnostic performance of the current ELISA kit.

ACKNOWLEDGMENTS

This work was supported in part by Protgen Ltd., which is a part of the National Engineering Laboratory for Anti-Tumor Protein Therapeutics (NEL), and the National Key R&D Program of China (Grant nos. 2016YFC0906000 and 2016YFC0906003). The sponsor had no role in study design, data collection, data analysis, data interpretation, and writing of the manuscript. Protgen Ltd. also provided the quantitative ELISA kit for measuring plasma Hsp90α. We greatly

thank the members of the Luo lab for insightful discussion and comments on the manuscript.

DISCLOSURE

The authors declared no conflict of interests.

ORCID

Yongzhang Luo https://orcid.org/0000-0002-2325-2329

REFERENCES

1. Marrugo-Ramirez J, Mir M, Samitier J. Blood-based cancer biomarkers in liquid biopsy: a promising non-invasive alternative to tissue biopsy. *Int J Med Sci*. 2018;19:2877-2898.
2. Bettegowda C, Sausen M, Leary RJ, et al. Detection of circulating tumor DNA in early- and late-stage human malignancies. *Sci Transl Med*. 2014;6(224):1-11.
3. Best MG, Sol N, Kooi IE, et al. RNA-Seq of tumor-educated platelets enables blood-based pan-cancer, multiclass, and molecular pathway cancer diagnostics. *Cancer Cell*. 2015;28(5):666-676.
4. Cohen JD, Li L, Wang Y, et al. Detection and localization of surgically resectable cancers with a multi-analyte blood test. *Science*. 2018;359(6378):926-930.
5. Li W, Tsen F, Sahu D, et al. Extracellular Hsp90 (eHsp90) as the actual target in clinical trials: intentionally or unintentionally. *Int Rev Cell Mol Biol*. 2013;303:203-235.
6. Chen JS, Hsu YM, Chen CC, et al. Secreted heat shock protein 90alpha induces colorectal cancer cell invasion through CD91/LRP-1 and NF-kappaB-mediated integrin alphaV expression. *J Biol Chem*. 2010;13(33):25458-25466.
7. Hance MW, Dole K, Gopal U, et al. Secreted Hsp90 is a novel regulator of the epithelial to mesenchymal transition (EMT) in prostate cancer. *J Biol Chem*. 2012;287(45):37732-37744.
8. Shi Y, Liu X, Lou J, et al. Plasma levels of heat shock protein 90 alpha associated with lung cancer development and treatment responses. *Clin Cancer Res*. 2014;20(23):6016-6022.
9. Fu Y, Xu X, Huang D, et al. Plasma heat shock protein 90alpha as a biomarker for the diagnosis of liver cancer: an official, large-scale, and multicenter clinical trial. *EBioMedicine*. 2017;24(C):56-63.
10. Lin XJ, Chong Y, Guo ZW, et al. A serum microRNA classifier for early detection of hepatocellular carcinoma: a multicentre, retrospective, longitudinal biomarker identification study with a nested case-control study. *Lancet Oncol*. 2015;16(7):804-815.
11. Dalerba P, Sahoo D, Paik S, et al. CDX2 as a prognostic biomarker in stage II and stage III colon cancer. *N Engl J Med*. 2016;374(3):211-222.
12. Gospodarowicz MK, Brierley JD, Wittekind C. *TNM Classification of Malignant Tumours*. London, UK: John Wiley & Sons; 2017.
13. Barrett T, Wilhite SE, Ledoux P, et al. NCBI GEO: archive for functional genomics data sets—update. *Nucleic Acids Res*. 2012;41:991-995.
14. Tripathi S, Pohl MO, Zhou Y, et al. Meta- and orthogonal integration of influenza "OMICs" data defines a role for UBR4 in virus budding. *Cell Host Microbe*. 2015;18(6):723-735.
15. Cock PJA, Fields CJ, Goto N, et al. The Sanger FASTQ file format for sequences with quality scores, and the Solexa/Illumina FASTQ variants. *Nucleic Acids Res*. 2010;38(6):1767-1771.
16. Langmead B, Trapnell C, Pop M, et al. Ultrafast and memory-efficient alignment of short DNA sequences to the human genome. *Genome Biol*. 2009;10(3):R25.
17. Kim D, Langmead B, Salzberg SL. HISAT: a fast spliced aligner with low memory requirements. *Nat Methods*. 2015;12(4):357-360.
18. Li B, Dewey CN. RSEM: accurate transcript quantification from RNA-seq data with or without a reference genome. *BMC Bioinformatics*. 2011;12(1):323.
19. Love MI, Huber W, Anders S. Moderated estimation of fold change and dispersion for RNA-seq data with DESeq2. *Genome Biol*. 2014;15(12):550.
20. Lu X, Wang X, Zhuo W, et al. The regulatory mechanism of a client kinase controlling its own release from Hsp90 chaperone machinery through phosphorylation. *Biochem J*. 2014;457(1):171-183.
21. Yang J, Liu W, Lu XA, et al. High expression of small GTPase Rab3D promotes cancer progression and metastasis. *Oncotarget*. 2015;6(13):11125-11138.
22. Worboys JD, Sinclair J, Yuan Y, et al. Systematic evaluation of quantotypic peptides for targeted analysis of the human kinome. *Nat Methods*. 2014;11(10):1041-1044.
23. Youden WJ. Index for rating diagnostic tests. *Cancer*. 1950;3(1):32-35.
24. Birrer RB, Birrer D, Klavins JV. Hepatocellular carcinoma and hepatitis virus. *Ann Clin Lab Sci*. 2003;33(1):39-54.
25. Khan SA, Davidson BR, Goldin R, et al. Guidelines for the diagnosis and treatment of cholangiocarcinoma: consensus document. *Gut*. 2002;51(suppl 6):VI1.
26. Hunter MC, Hagan KLO, Kenyon A, et al. Hsp90 binds directly to fibronectin (FN) and inhibition reduces the extracellular fibronectin matrix in breast cancer cells. *PLoS ONE*. 2014;9(1):e86842.
27. Song X, Wang X, Zhuo W, et al. The regulatory mechanism of extracellular Hsp90α on matrix metalloproteinase-2 processing and tumor angiogenesis. *J Biol Chem*. 2010;17(51):40039-40049.
28. Eustace BK, Sakurai T, Stewart JK, et al. Functional proteomic screens reveal an essential extracellular role for hsp90[alpha] in cancer cell invasiveness. *Nat Cell Biol*. 2004;6(6):507-514.
29. Cheng C, Fan J, Fedesco M, et al. Transforming growth factorα(TGFα)-stimulated secretion of HSP90α: using the receptor LRP-1/CD91 to promote human skin cell migration against a TGF?-rich environment during wound healing. *Mol Cell Biol*. 2008;28(10):3344-3358.
30. Mccready J, Sims JD, Chan D, et al. Secretion of extracellular hsp90α via exosomes increases cancer cell motility: a role for plasminogen activation. *BMC Cancer*. 2010;10(1):294.
31. Seegar TC, Killingsworth LB, Saha N, et al. Structural basis for regulated proteolysis by the α-secretase ADAM10. *Cell*. 2017;171(7):1638-1648. e7.
32. Jones AV, Lambert DW, Speight PM, et al. ADAM 10 is over expressed in oral squamous cell carcinoma and contributes to invasive behaviour through a functional association with αvβ6 integrin. *FEBS Lett*. 2013;587(21):3529-3534.
33. Wang Y, Ye Z, Li L, et al. ADAM 10 is associated with gastric cancer progression and prognosis of patients. *J Surg Oncol*. 2011;103(2):116-123.
34. Huovila AP, Turner AJ, Pelto-Huikko M, et al. Shedding light on ADAM metalloproteinases. *Trends Biochem Sci*. 2005;30(7):413-422.
35. Anders A, Gilbert S, Garten W, et al. Regulation of the α-secretase ADAM10 by its prodomain and proprotein convertases. *FASEB J*. 2001;15(10):1837-1839.
36. Wang X, Song X, Zhuo W, et al. The regulatory mechanism of Hsp90α secretion and its function in tumor malignancy. *Proc Natl Acad Sci USA*. 2009;106(50):21288-21293.
37. Li D, Mallory T, Satomura S. AFP-L3: a new generation of tumor marker for hepatocellular carcinoma. *Clin Chim Acta*. 2001;313:15-19.
38. Moulick K, Ahn JH, Zong H, et al. Affinity-based proteomics reveal cancer-specific networks coordinated by Hsp90. *Nat Chem Biol*. 2011;7:818.
39. Rodina A, Wang T, Yan P, et al. The epichaperome is an integrated chaperome network that facilitates tumour survival. *Nature*. 2016;538:397.

40. Pan S, Chen R, Brand RE, et al. Multiplex targeted proteomic assay for biomarker detection in plasma: a pancreatic cancer biomarker case study. *J Proteome Res*. 2012;11(3):1937-1948.
41. Keshishian H, Addona T, Burgess M, et al. Quantitative, multiplexed assays for low abundance proteins in plasma by targeted mass spectrometry and stable isotope dilution. *Mol Cell Proteomics*. 2007;6(12):2212-2229.
42. Meacham CE, Morrison SJ. Tumour heterogeneity and cancer cell plasticity. *Nature*. 2013;501(7467):328.
43. Li W, Li Y, Guan S, et al. Extracellular heat shock protein-90α: linking hypoxia to skin cell motility and wound healing. *EMBO J*. 2007;26(5):1221-1233.
44. Yang Y, Rao R, Shen J, et al. Role of acetylation and extracellular location of heat shock protein 90α in tumor cell invasion. *Cancer Res*. 2008;68(12):4833-4842.
45. Elaimy AL, Ahsan A, Marsh K, et al. ATM is the primary kinase responsible for phosphorylation of Hsp90α after ionizing radiation. *Oncotarget*. 2016;7(50):82450.
46. Lees-Miller SP, Anderson CW. The human double-stranded DNA-activated protein kinase phosphorylates the 90-kDa heat-shock protein, hsp90 alpha at two NH2-terminal threonine residues. *J Biol Chem*. 1989;264(29):17275-17280.
47. Wang X, Lu X, Song X, et al. Thr90 phosphorylation of Hsp90α by protein kinase A regulates its chaperone machinery. *Biochem J*. 2012;441(1):387-397.
48. Whitesell L, Lindquist S. HSP90 and the chaperoning of cancer. *Nat Rev Cancer*. 2005;5(10):761-772.
49. Li W, Sahu D, Tsen F. Secreted heat shock protein-90 (Hsp90) in wound healing and cancer. *Biochim Biophys Acta*. 2012;1823(3):730-741.
50. Wong DS, Jay DG. Emerging roles of extracellular Hsp90 in cancer. *Adv Cancer Res*. 2016;129:141.
51. Kaplan RN, Riba RD, Zacharoulis S, et al. VEGFR1-positive haematopoietic bone marrow progenitors initiate the pre-metastatic niche. *Nat Med*. 2005;438(7069):820-827.
52. Huang Y, Song N, Ding Y, et al. Pulmonary vascular destabilization in the premetastatic phase facilitates lung metastasis. *Cancer Res*. 2009;69(19):7529-7537.
53. Neckers L, Workman P. Hsp90 molecular chaperone inhibitors: are we there yet? *Clin Cancer Res*. 2012;18(1):64-76.
54. Hanahan D, Weinberg RA. Hallmarks of cancer: the next generation. *Cell*. 2011;144(5):646-674.
55. Gutwein P, Mechtersheimer S, Riedle S, et al. ADAM10-mediated cleavage of L1 adhesion molecule at the cell surface and in released membrane vesicles. *FASEB J*. 2002;17(2):292-294.
56. Mathews J, Gibb DR, Chen B, et al. CD23 Sheddase A disintegrin and metalloproteinase 10 (ADAM10) is also required for CD23 sorting into B cell-derived exosomes. *J Biol Chem*. 2010;285(48):37531-37541.
57. Koivunen J, Aaltonen V, Peltonen J. Protein kinase C (PKC) family in cancer progression. *Cancer Lett*. 2006;235:1-10.
58. Wu D, Struwe WB, Harvey DJ, et al. N-glycan microheterogeneity regulates interactions of plasma proteins. *Proc Natl Acad Sci USA*. 2018;115(35):8763-8768.
59. Mollapour M, Tsutsumi S, Truman AW, et al. Threonine 22 phosphorylation attenuates Hsp90 interaction with cochaperones and affects its chaperone activity. *Mol Cell*. 2011;41(6):672-681.
60. Mollapour M, Tsutsumi S, Donnelly AC, et al. Swe1Wee1-dependent tyrosine phosphorylation of Hsp90 regulates distinct facets of chaperone function. *Mol Cell*. 2010;37(3):333-343.

SUPPORTING INFORMATION

Additional supporting information may be found online in the Supporting Information section at the end of the article.

How to cite this article: Liu W, Li J, Zhang P, et al. A novel pan-cancer biomarker plasma heat shock protein 90alpha and its diagnosis determinants in clinic. *Cancer Sci*. 2019;110:2941-2959. https://doi.org/10.1111/cas.14143